Realization of a Townes Soliton in a Two-Component Planar Bose Gas

B. Bakkali-Hassani,[1] C. Maury,[1] Y.-Q. Zou,[1] É. Le Cerf,[1] R. Saint-Jalm,[3] P. C. M. Castilho,[2] S. Nascimbene,[1] J. Dalibard,[1] and J. Beugnon[1]

[1]*Laboratoire Kastler Brossel, Collège de France, CNRS, ENS-PSL University, Sorbonne Université, 11 Place Marcelin Berthelot, 75005 Paris, France*

[2]*Instituto de Física de São Carlos, Universidade de São Paulo, CP 369, 13560-970 São Carlos, Brazil*

[3]*Department of Physics, Ludwig-Maximilians-Universität München, Schellingstrasse 4, D-80799 München, Germany*

(Received 4 March 2021; revised 7 May 2021; accepted 24 May 2021; published 9 July 2021)

Most experimental observations of solitons are limited to one-dimensional (1D) situations, where they are naturally stable. For instance, in 1D cold Bose gases, they exist for any attractive interaction strength g and particle number N. By contrast, in two dimensions, solitons appear only for discrete values of gN, the so-called Townes soliton being the most celebrated example. Here, we use a two-component Bose gas to prepare deterministically such a soliton: Starting from a uniform bath of atoms in a given internal state, we imprint the soliton wave function using an optical transfer to another state. We explore various interaction strengths, atom numbers, and sizes and confirm the existence of a solitonic behavior for a specific value of gN and arbitrary sizes, a hallmark of scale invariance.

DOI: 10.1103/PhysRevLett.127.023603

Solitary waves are encountered in a broad range of fields, including photonics, hydrodynamics, condensed matter, and high-energy physics [1]. The solitonic behavior usually originates from the balance between the tendency to expansion of a wave packet in a dispersive medium and a nonlinear contracting effect. For a real or complex field ϕ in dimension D, a paradigm example is provided by the energy functional

$$E[\phi] = \frac{1}{2}\int d^D r[|\nabla\phi(\boldsymbol{r})|^2 - G|\phi(\boldsymbol{r})|^4], \tag{1}$$

where G is a real positive parameter and ϕ is normalized to unity ($\int d^D r|\phi|^2 = 1$). This energy functional is relevant for describing the propagation of an intense laser beam in a nonlinear cubic medium, where diffraction and self-focusing compete. It is also used to model the evolution of coherent matter waves when the kinetic energy contribution competes with attractive interactions.

Experimentally, most studies concentrate on effective one-dimensional situations, as solitons in higher dimensions are more prone to instabilities and then much more challenging to investigate experimentally [2]. This can be understood from a simple scaling analysis of $E[\phi]$, assuming a wave packet ϕ of size ℓ,

$$E(\ell) \sim \frac{1}{\ell^2} - \frac{G}{\ell^D}. \tag{2}$$

For $D = 1$, this leads to a stable minimum for $\ell^* \sim 1/G$, whereas for $D = 3$, the extremum obtained for $\ell^* \sim G$ is dynamically unstable.

The case $D = 2$ is of specific interest because the two terms of the estimate of Eq. (2) scale as $1/\ell^2$. The existence of a localized wave packet minimizing $E[\phi]$ (or more generally making it stationary) can thus be achieved only for discrete values of G. The Townes soliton, introduced in Ref. [3], is a celebrated example of such a stationary state. It is the real, nodeless, and axially symmetric solution of the two-dimensional (2D) Gross-Pitaevskii or nonlinear Schrödinger equation (NLSE) obtained by imposing $\delta E[\phi] = 0$,

$$-\frac{1}{2}\nabla^2\phi(\boldsymbol{r}) - G\phi^3(\boldsymbol{r}) = \mu\phi(\boldsymbol{r}), \tag{3}$$

where the chemical potential μ can take any negative value. These solutions, which have zero energy ($E[\phi] = 0$), exist only for $G = G_T \approx 5.85$. Scale invariance of the 2D NLSE [4] provides a relation between them: if $\phi(\boldsymbol{r})$ is a solution of Eq. (3) for a given μ, then for any real λ, $\lambda\phi(\lambda\boldsymbol{r})$ is also a normalized solution with a rescaled μ, still with zero energy. For $G < G_T$, there are no stationary localized solutions of Eq. (3), while for $G > G_T$, one can find localized functions ϕ with an arbitrarily large and negative energy $E[\phi]$.

Townes solitons have been mostly investigated in nonlinear optics where the cubic term in Eq. (3) corresponds to a Kerr nonlinearity that induces self-focusing for intense enough beams [5–7]. The soliton solution then corresponds to a specific optical power. Numerous strategies have been developed to stabilize the Townes soliton and to observe some features of solitonic propagation in various optical settings [8–14]. Ultracold gases are another well-known

platform to investigate soliton physics in 1D [15–19]. The 2D case has been recently explored in Ref. [20] using a quench of the interaction strength to negative values. The formation of multiple stationary wave packets was observed, where the size of a wave packet was fixed by the out-of-equilibrium dynamics.

In this Letter, we report the first deterministic realization of a 2D matter-wave Townes soliton. We demonstrate, at a given interaction strength, the existence of stationary states for a well-defined atom number and for the specific "Townes profile" of the density distribution. We also show that this behavior is independent of the wave packet size, hence confirming scale invariance. To produce this soliton, we use a novel approach based on a two-component Bose gas for which the equilibrium state of one minority component immersed in a bath defined by the other component is well described, in the weak depletion regime, by an effective single-component NLSE with cubic nonlinearity.

We consider atoms of mass m in states $|1\rangle$ and $|2\rangle$ with repulsive contact interactions. The intracomponent ($\tilde{g}_{11}$, $\tilde{g}_{22}$) and the intercomponent ($\tilde{g}_{12}$) interaction parameters are thus all positive. Such a mixture is well described in the zero-temperature limit by two coupled NLSEs. In the weak depletion regime, one can assume that the dynamics of the dense bath of atoms in state $|1\rangle$ with density n_1 occurs on a short timescale [$\propto m/(\hbar^2\tilde{g}_{11}n_1)$] compared to the minority component dynamics. The bath is then always at equilibrium on the timescale of the evolution of the minority component. The equilibrium state $\phi(\boldsymbol{r})$ for N particles in state $|2\rangle$ then satisfies the single-component NLSE given in Eq. (3) with

$$G = -N\tilde{g}_e, \qquad \tilde{g}_e = \tilde{g}_{22} - \frac{\tilde{g}_{12}^2}{\tilde{g}_{11}}. \tag{4}$$

The effective interaction parameter $\tilde{g}_e$ corresponds to a dressing of the interactions for component $|2\rangle$ by the bath [21]. In this limit, the dynamics of the particles in state $|2\rangle$ remains scale invariant since the characteristic length of the bath, i.e., its healing length, does not play any role. We discuss at the end of this Letter possible deviations from this limit.

The experiments described in this Letter focus on the case of ^{87}Rb atoms in their electronic ground level, where all interaction parameters $\tilde{g}_{ij}$ are close to each other within a few percent. Here we use the $|1\rangle = |F = 1, m_F = 0\rangle$ and $|2\rangle = |F = 2, m_F = 0\rangle$ states for which we have $\tilde{g}_e < 0$. The negative value of $\tilde{g}_e$ implies that the effective dynamics of the minority component is akin to the one of a gas with attractive interactions, as required for observing Townes solitons. The condition for effective attractive interactions is also equivalent to the immiscibility criterion for the two components [22]. The atom number N_T corresponding to the Townes soliton for a cloud with interaction parameter $\tilde{g}_e$ is then given by $N_T = G_T/|\tilde{g}_e|$.

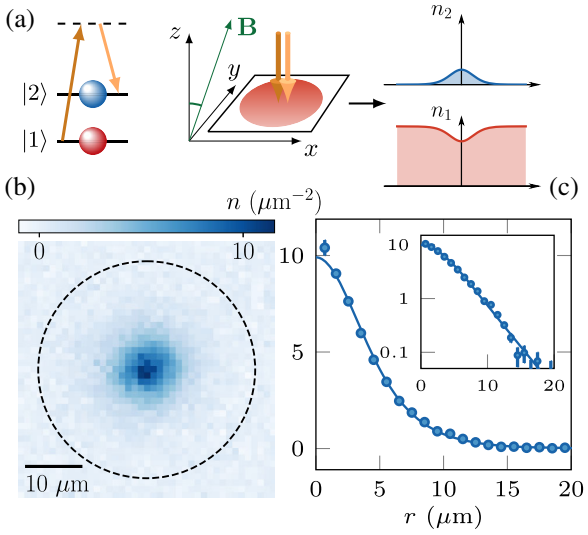

FIG. 1. (a) Schematics of the experiment. We create a disk-shaped planar Bose gas in the xy plane in state $|1\rangle$. At time $t = 0$ we pulse a pair of copropagating Raman beams that transfer in a spatially resolved way a small fraction of the atoms from state $|1\rangle$ to state $|2\rangle$. An example of density distribution $n_2 \equiv n$ in state $|2\rangle$ obtained when preparing a Townes profile is shown in (b); the dashed line indicates the edge of the bath of atoms in state $|1\rangle$. Its radial profile is reported in (c) as blue dots, together with its fit to a Townes density profile (solid line). Inset: displays the same data in semilog scale highlighting the approximately exponential tails of the Townes profile.

Our experimental study of Townes solitons starts with the preparation of a uniform two-dimensional Bose gas of ^{87}Rb atoms in state $|1\rangle$, as detailed in Refs. [23,24]. Atoms are confined in a circularly shaped box potential in the horizontal plane and they occupy the ground state of an approximately harmonic potential along the vertical direction. The typical cloud temperature is < 20 nK and the column density is set around 100 atoms/μm^2. In this regime, the gas is well described by a 2D cubic NLSE. An external magnetic field of 0.7 G with tunable orientation is applied.

At time $t = 0$, we create a custom-shaped wave packet of atoms in component $|2\rangle$ immersed in a bath of atoms in component $|1\rangle$, as shown in Fig. 1(a). This is achieved by transferring, in a spatially resolved way, a controlled fraction of atoms into $|2\rangle$ thanks to a two-photon Raman transition, which keeps the total density constant. We use two collinear laser beams so as not to impart any significant momentum to the transferred atoms. The in plane intensity profile of these beams is shaped by a spatial light modulator, which allows us to design arbitrary intensity patterns on the atomic cloud with about 1 μm spatial resolution [25,27]. We show in Figs. 1(b) and 1(c) an example realization of a Townes profile, i.e., a density distribution $n(\boldsymbol{r})$ proportional to $|\phi(\boldsymbol{r})|^2$, where ϕ is obtained by a numerical resolution of Eq. (3). It shows an excellent control of the density distribution of

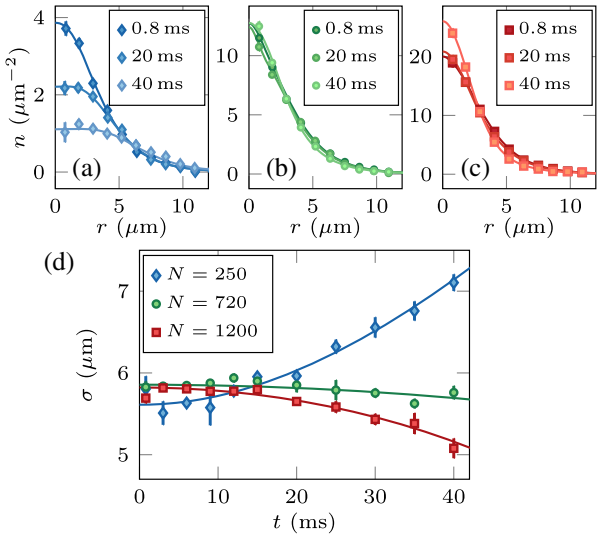

FIG. 2. (a)–(c) Radial profiles at different times for imprinted Townes profiles with (a) $N = 250(40)$, (b) $N = 720(20)$, and (c) $N = 1200(50)$ atoms. Initial rms sizes are similar and the magnetic field is perpendicular to the atomic plane. The solid lines are fits to the data. (d) Time evolution of the fitted rms size for the same three configurations. The solid lines are a fit to the data with Eq. (6). Note that, for N notably different from N_T, the functional form of the density distribution $n(r)$ changes significantly during the evolution. Therefore, the product $n(0)\sigma^2$ is not a constant of motion in spite of the atom number conservation (see Supplemental Material [25] for details).

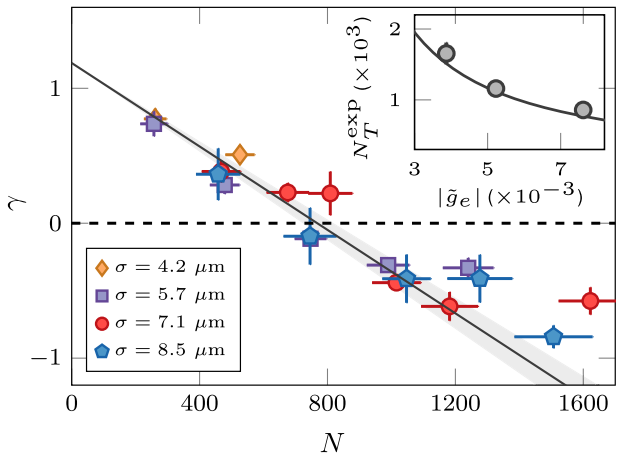

FIG. 3. Expansion coefficient as a function of the atom number of the imprinted wave packet for a magnetic field perpendicular to the atomic plane. All data for different initial sizes collapse onto a single curve. The solid line is the theory prediction computed for $\tilde{g}_e = -7.6 \times 10^{-3}$ without any adjustable parameter. The shaded area around this line represents our estimated uncertainty on the calibration of $\tilde{g}_e$. Inset: variation of the experimentally determined stationary atom number $N_T^{\rm exp}$ for different values of $\tilde{g}_e$. The stationary atom number is determined from a linear fit of the various $\gamma(N)$ curves [25]. The solid line is the prediction $N_T = G_T/|\tilde{g}_e|$.

component $|2\rangle$ over more than two decades in density. After imprinting a Townes profile of given amplitude and width, we let the system evolve and we measure the *in situ* density distribution via absorption imaging. All the profiles studied here are initially in the weak depletion regime, where the density n does not exceed 20% of the bath density. We restrict the time evolution to durations short enough to limit the amount of losses in state $|2\rangle$, essentially due to hyperfine relaxation, to typically $\lesssim$10%.

The two states used in this Letter are characterized by their s-wave scattering lengths $a_{11} = 100.9a_0$, $a_{22} - a_{11} = -6.0a_0$, and $a_{12} - a_{11} = -2.0a_0$ [28], where a_0 is the Bohr radius. Thanks to the existence of magnetic dipole-dipole interactions in a mixture of the two components, the value of a_{12} can be shifted, for a 2D cloud, by an amount varying from $-0.7a_0$ to $+1.4a_0$ by changing the angle of the applied magnetic field with respect to the atomic plane [29]. In all cases, we have $a_{22} - a_{12}^2/a_{11} < 0$ and thus a similar inequality for the interaction parameters defined as $\tilde{g}_{ij} = \sqrt{8\pi}a_{ij}/\ell_z$ for $i, j = 1, 2$, where $\ell_z = \sqrt{\hbar/m\omega_z}$ is the harmonic oscillator length associated with the confinement along the vertical direction of frequency ω_z. Here, we have $\tilde{g}_{11} = 0.16(1)$.

In Figs. 2(a)–2(c), we show, for three different atom numbers, the measured time evolution of a Townes profile with a root mean square (rms) size at time $t = 0$ given by $\sigma_0 = 5.7$ μm and the external magnetic field perpendicular to the atomic plane ($\tilde{g}_e \approx -7.6 \times 10^{-3}$). We observe an almost stationary time evolution for $N = 720(20)$, whereas the central density of the cloud decreases for $N = 250(40)$ and increases for $N = 1200(50)$. More quantitatively, for each time t we extract the rms size $\sigma(t)$ of the cloud (see Supplemental Material [25] for details) and we study its time evolution, as shown in Fig. 2(d).

We analyze these data using the variance identity (or virial theorem), which provides the time evolution of the rms size of the density profile for the 2D NLSE [4]

$$\frac{d^2\sigma^2}{dt^2} = \frac{4E}{m}, \tag{5}$$

where E is the total (kinetic + interaction) energy per particle. We thus fit the time evolution of σ to the function resulting from the integration of Eq. (5)

$$\sigma^2(t) = \sigma_0^2 + \left(\frac{\hbar}{m\sigma_0}\right)^2 \gamma t^2, \tag{6}$$

where we assumed that the imprinted state is a real wave function and thus $d\sigma/dt = 0$ at $t = 0$. For the Townes profile, one can show that the explicit expressions of the kinetic and interaction energy integrals lead to $\gamma = \alpha(1 - N/N_T)$, where $\alpha \approx 1.19$ is determined numerically (note that $\gamma = 1$ for a noninteracting Gaussian wave packet).

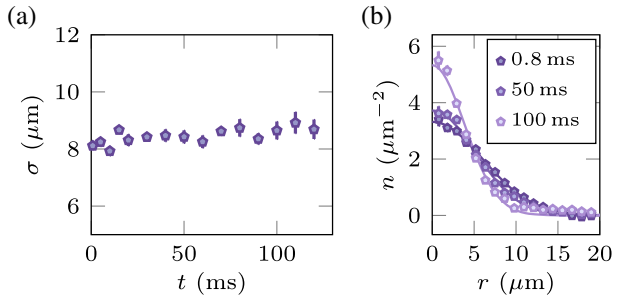

FIG. 4. Time evolution of a Gaussian profile with $N \sim 800 \sim N_G$. (a) The chosen atom number corresponds to a zero energy state as shown by the almost stationary rms size. However, the density profile shown in (b) evolves with time in contrast to the Townes profile shown in Fig. 2(b).

We report in Fig. 3 the fitted expansion coefficient γ as a function of the atom number N for different values of the initial size σ_0. All data collapse onto a single curve $\gamma(N)$, which experimentally confirms the scale invariance of the system. The stationary state $\gamma = 0$ is obtained for $N_T^{\mathrm{exp}} = 790(40)$ (determined with a linear fit). We also show as a solid line the prediction $\gamma = \alpha(1 - N/N_T)$, where $N_T = 770(50)$ is fixed by the independently estimated value of $\tilde{g}_e$ [30]. It shows a very good agreement for lower values of N. The small deviation at large N is likely due to the larger density of the minority component wave packet, which leads to increased losses and deviation from the low depletion regime.

The relevant quantity to determine the behavior of the imprinted wave packet is $|\tilde{g}_e|N$ that should be compared to $G_T = 5.85$. We show in the inset of Fig. 3 the measured variation of N_T^{exp} when varying the orientation of the applied magnetic field with respect to the atomic plane and hence the interspecies scattering length. We confirm the prediction $N_T = G_T/|\tilde{g}_e|$, with $\tilde{g}_e$ varying from -3.9×10^{-3} to -7.6×10^{-3} [25,29].

For an arbitrary density profile there always exists an atom number such that the energy of Eq. (1) is zero and hence, from Eq. (5), the rms size is stationary. Of course, this is not sufficient to achieve a fully stationary profile. We illustrate this point in Fig. 4 for the case of an initial Gaussian profile, for which a zero energy is obtained for $N_G = 2\pi/|\tilde{g}_e|$ [31]. We check in Fig. 4(a) that this number leads to a stationary rms. However, the observed density distribution is clearly not stationary, as shown in Fig. 4(b).

Our approach using a two-component gas raises new specific questions. For instance, for a wave packet with large enough G, the central density can diverge at a finite time in the single-component case, whereas such a collapsing behavior cannot occur in the two-component case with repulsive interactions (all $\tilde{g}_{ij} > 0$). Indeed, as the minority component density becomes comparable to the bath one, the bath brings a new length scale to the effective one-component description, thus breaking scale invariance. Let us briefly discuss this problem in the case of close interaction parameters $\tilde{g}_{ij}$, which is relevant for the two states of ^{87}Rb used here. In this limit, the coupled NLSEs describing the binary system can be simplified into a single one describing the equilibrium state of component $|2\rangle$, without requiring a weak depletion approximation [25]. Introducing the bath density n_∞, we expand this single-component equation at first order ϕ^2/n_∞ and obtain

$$-\frac{1}{2}\nabla^2\phi - G\phi^3 - \frac{N}{4}\frac{(\nabla^2\phi^2)}{n_\infty}\phi = \mu\phi. \tag{7}$$

We recover Eq. (3) with the same effective interaction parameter $G = -N\tilde{g}_e$, but with an additional stabilizing term that breaks scale invariance. The influence of this term was investigated in a different context in Ref. [32]. Contrary to the case of the cubic equation, it leads for any atom number $N > N_T$ to a localized ground-state solution with a well-defined size σ_N. We checked that for all data reported in Fig. 3 the shift of the stationary atom number due to the additional stabilizing term of Eq. (7) remains small ($\lesssim 10\%$) (see Supplemental Material [25]).

Scale invariance is also broken in the one-component case when one regularizes the contact potential that leads to the interaction energy term $-G\int|\phi|^4$ in Eq. (1) [33–35]. Such a regularization is not required as long as one restricts to the classical field approach of Eqs. (1) and (4), valid for $|\tilde{g}_e| \ll 1$ [36], but it becomes compulsory for larger $|\tilde{g}_e|$, where a quantum treatment of atomic interactions is in order. After regularization, the interaction strength $\tilde{g}_e$ becomes a running coupling constant. Then, there exists a stable solution of size σ_N and energy E_N for any value of the atom number N with the geometric scaling $\sigma_{N+1}/\sigma_N \approx 0.34$ [33]. In practice, the predicted value for σ_N is physically reasonable only for $|N - N_T| \sim$ few units. Moreover, for $|\tilde{g}_e| \lll 1$, as explored here, the typical evolution timescale of a N-particle state with a Townes profile of size σ slightly different from σ_N will be prohibitively long [25]. In the case $|\tilde{g}_e| \sim 1$, a realistic droplet size would be achieved for only a few atoms and one could observe the predicted scaling of σ_N with N.

It is also interesting to put our work in perspective with the physics of quantum droplets [37,38] or mixed bubbles [39], which has recently attracted great interest. Such droplets have been observed in 1D or 3D geometries [40–45]. Their formation results from the competition between a tunable mean-field attractive term and a beyond-mean-field repulsive term. The scaling of the two terms with density is different and leads to a stable equilibrium with a droplet size that depends on the particle number. In this Letter, the observed 2D solitons are purely mean-field objects resulting from the balance between effective attractive interactions and kinetic energy.

To summarize, we have presented a new platform to explore the physics of solitons in two dimensions. Higher

order solutions of the 2D NLSE, with nodes in the density profile [46,47] or vortex solitons [48], can also be investigated with similar methods. Another natural extension consists in printing solitons with a well-defined momentum imparted by the two-photon Raman transfer. Propagation, interaction, or fusion of solitons could then be explored [49–52]. Additionally, whereas we focused here on the equilibrium solution at zero temperature, it will be interesting to study the elementary excitations of these solitons [53], as well as the role of finite temperature on the dynamical behavior of these objects [54].

This work is supported by ERC (Synergy UQUAM), European Union's Horizon 2020 Programme (QuantERA NAQUAS project), and the ANR-18-CE30-0010 grant. We thank D. Petrov for fruitful discussions and G. Chauveau for his participation to the final stage of the project.

Note added.—Recently, a study about the scale invariance of isolated 2D solitary waves emerging from a modulational instability in an attractive atomic Bose gas was reported in [55].

[1] T. Dauxois and M. Peyrard, *Physics of Solitons* (Cambridge University Press, Cambridge, 2006).
[2] Y. V. Kartashov, G. E. Astrakharchik, B. A. Malomed, and L. Torner, Frontiers in multidimensional self-trapping of nonlinear fields and matter, Nat. Rev. Phys. **1**, 185 (2019).
[3] R. Y. Chiao, E. Garmire, and C. H. Townes, Self-Trapping of Optical Beams, Phys. Rev. Lett. **13**, 479 (1964).
[4] L. P. Pitaevskii and A. Rosch, Breathing modes and hidden symmetry of trapped atoms in two dimensions, Phys. Rev. A **55**, R853 (1997).
[5] J. E. Bjorkholm and A. A. Ashkin, CW Self-Focusing and Self-Trapping of Light in Sodium Vapor, Phys. Rev. Lett. **32**, 129 (1974).
[6] A. Barthelemy, S. Maneuf, and C. Froehly, Propagation soliton et auto-confinement de faisceaux laser par non linearité optique de Kerr, Opt. Commun. **55**, 201 (1985).
[7] K. D. Moll, A. L. Gaeta, and G. Fibich, Self-Similar Optical Wave Collapse: Observation of the Townes Profile, Phys. Rev. Lett. **90**, 203902 (2003).
[8] W. E. Torruellas, Z. Wang, D. J. Hagan, E. W. VanStryland, G. I. Stegeman, L. Torner, and C. R. Menyuk, Observation of Two-Dimensional Spatial Solitary Waves in a Quadratic Medium, Phys. Rev. Lett. **74**, 5036 (1995).
[9] E. L. Falcão Filho, C. B. de Araújo, G. Boudebs, H. Leblond, and V. Skarka, Robust Two-Dimensional Spatial Solitons in Liquid Carbon Disulfide, Phys. Rev. Lett. **110**, 013901 (2013).
[10] A. S. Reyna, K. C. Jorge, and C. B. de Araújo, Two-dimensional solitons in a quintic-septimal medium, Phys. Rev. A **90**, 063835 (2014).
[11] G. C. Duree, J. L. Shultz, G. J. Salamo, M. Segev, A. Yariv, B. Crosignani, P. Di Porto, E. J. Sharp, and R. R. Neurgaonkar, Observation of Self-Trapping of an Optical Beam Due to the Photorefractive Effect, Phys. Rev. Lett. **71**, 533 (1993).
[12] A. Pasquazi, S. Stivala, G. Assanto, J. Gonzalo, J. Solis, and C. N. Afonso, Near-infrared spatial solitons in heavy metal oxide glasses, Opt. Lett. **32**, 2103 (2007).
[13] J. W. Fleischer, M. Segev, N. K. Efremidis, and D. N. Christodoulides, Observation of two-dimensional discrete solitons in optically induced nonlinear photonic lattices, Nature (London) **422**, 147 (2003).
[14] E. A. Cerda-Méndez, D. Sarkar, D. N. Krizhanovskii, S. S. Gavrilov, K. Biermann, M. S. Skolnick, and P. V. Santos, Exciton-Polariton Gap Solitons in Two-Dimensional Lattices, Phys. Rev. Lett. **111**, 146401 (2013).
[15] S. Burger, K. Bongs, S. Dettmer, W. Ertmer, K. Sengstock, A. Sanpera, G. V. Shlyapnikov, and M. Lewenstein, Dark Solitons in Bose-Einstein Condensates, Phys. Rev. Lett. **83**, 5198 (1999).
[16] J. Denschlag, J. E. Simsarian, D. L. Feder, C. W. Clark, L. A. Collins, J. Cubizolles, L. Deng, E. W. Hagley, K. Helmerson, W. P. Reinhardt, S. L. Rolston, B. I. Schneider, and W. D. Phillips, Generating solitons by phase engineering of a Bose-Einstein condensate, Science **287**, 97 (2000).
[17] L. Khaykovich, F. Schreck, G. Ferrari, T. Bourdel, J. Cubizolles, L. D. Carr, Y. Castin, and C. Salomon, Formation of a matter-wave bright soliton, Science **296**, 1290 (2002).
[18] K. E. Strecker, G. B. Partridge, A. G. Truscott, and R. G. Hulet, Formation and propagation of matter-wave soliton trains, Nature (London) **417**, 150 (2002).
[19] B. Eiermann, Th. Anker, M. Albiez, M. Taglieber, P. Treutlein, K.-P. Marzlin, and M. K. Oberthaler, Bright Bose-Einstein Gap Solitons of Atoms with Repulsive Interaction, Phys. Rev. Lett. **92**, 230401 (2004).
[20] C.-A. Chen and C.-L. Hung, Observation of Universal Quench Dynamics and Townes Soliton Formation from Modulational Instability in Two-Dimensional Bose Gases, Phys. Rev. Lett. **125**, 250401 (2020).
[21] C. J. Pethick and H. Smith, *Bose-Einstein Condensation in Dilute Gases* (Cambridge University Press, Cambridge, 2008).
[22] E. Timmermans, Phase Separation of Bose-Einstein Condensates, Phys. Rev. Lett. **81**, 5718 (1998).
[23] J. L. Ville, T. Bienaimé, R. Saint-Jalm, L. Corman, M. Aidelsburger, L. Chomaz, K. Kleinlein, D. Perconte, S. Nascimbène, J. Dalibard, and J. Beugnon, Loading and compression of a single two-dimensional Bose gas in an optical accordion, Phys. Rev. A **95**, 013632 (2017).
[24] R. Saint-Jalm, P. C. M. Castilho, É. Le Cerf, B. Bakkali-Hassani, J.-L. Ville, S. Nascimbene, J. Beugnon, and J. Dalibard, Dynamical Symmetry and Breathers in a Two-Dimensional Bose Gas, Phys. Rev. X **9**, 021035 (2019).
[25] See Supplemental Material at http://link.aps.org/supplemental/10.1103/PhysRevLett.127.023603 for methods, complementary data and theoretical discussions, which includes Ref. [26].
[26] V. E. Zakharov, Instability of self-focusing of light, Sov. Phys. JETP **26**, 994 (1968), http://www.jetp.ac.ru/cgi-bin/e/index/e/26/5/p994?a=list.
[27] Y. Zou, E. Le Cerf, B. Bakkali-Hassani, C. Maury, G. Chauveau, P. C. M. Castilho, R. Saint-Jalm, S. Nascimbene, J. Dalibard, and J. Beugnon, Optical control of the density and spin spatial profiles of a planar Bose gas, J. Phys. B **54**, 08LT01 (2021).

[28] P. A. Altin, G. McDonald, D. Döring, J. E. Debs, T. H. Barter, J. D. Close, N. P. Robins, S. A. Haine, T. M. Hanna, and R. P. Anderson, Optically trapped atom interferometry using the clock transition of large ^{87}Rb Bose-Einstein condensates, New J. Phys. **13**, 065020 (2011).

[29] Y.-Q. Zou, B. Bakkali-Hassani, C. Maury, É. Le Cerf, S. Nascimbene, J. Dalibard, and J. Beugnon, Magnetic Dipolar Interaction between Hyperfine Clock States in a Planar Alkali Bose Gas, Phys. Rev. Lett. **125**, 233604 (2020).

[30] The reported uncertainties on the measured atom number are associated with the statistical variations of the cloud over the different repetitions of the experiment. Systematic errors on the atom number calibration are estimated to be on the order of 10%. The determination of N_T is sensitive to the knowledge of the scattering length differences. A variation of these two differences by $0.1a_0$ corresponds to a variation of N_T by ≈50 atoms for our experimental parameters.

[31] G. Fibich and A. L. Gaeta, Critical power for self-focusing in bulk media and in hollow waveguides, Opt. Lett. **25**, 335 (2000).

[32] N. N. Rosanov, A. G. Vladimirov, D. V. Skryabin, and W. J. Firth, Internal oscillations of solitons in two-dimensional NLS equation with nonlocal nonlinearity, Phys. Lett. A **293**, 45 (2002).

[33] H.-W. Hammer and D. T. Son, Universal Properties of Two-Dimensional Boson Droplets, Phys. Rev. Lett. **93**, 250408 (2004).

[34] D. Lee, Large-N droplets in two dimensions, Phys. Rev. A **73**, 063204 (2006).

[35] B. Bazak and D. S. Petrov, Energy of N two-dimensional bosons with zero-range interactions, New J. Phys. **20**, 023045 (2018).

[36] B. V. Svistunov, E. S. Babaev, and N. V. Prokof'ev, *Superfluid States of Matter* (CRC Press, Boca Raton, 2015).

[37] A. Bulgac, Dilute Quantum Droplets, Phys. Rev. Lett. **89**, 050402 (2002).

[38] D. S. Petrov, Quantum Mechanical Stabilization of a Collapsing Bose-Bose Mixture, Phys. Rev. Lett. **115**, 155302 (2015).

[39] P. Naidon and D. S. Petrov, Mixed Bubbles in Bose-Bose Mixtures, Phys. Rev. Lett. **126**, 115301 (2021).

[40] M. Schmitt, M. Wenzel, F. Böttcher, I. Ferrier-Barbut, and T. Pfau, Self-bound droplets of a dilute magnetic quantum liquid, Nature (London) **539**, 259 (2016).

[41] I. Ferrier-Barbut, H. Kadau, M. Schmitt, M. Wenzel, and T. Pfau, Observation of Quantum Droplets in a Strongly Dipolar Bose Gas, Phys. Rev. Lett. **116**, 215301 (2016).

[42] L. Chomaz, S. Baier, D. Petter, M. J. Mark, F. Wächtler, L. Santos, and F. Ferlaino, Quantum-Fluctuation-Driven Crossover from a Dilute Bose-Einstein Condensate to a Macrodroplet in a Dipolar Quantum Fluid, Phys. Rev. X **6**, 041039 (2016).

[43] C. R. Cabrera, L. Tanzi, J. Sanz, B. Naylor, P. Thomas, P. Cheiney, and L. Tarruell, Quantum liquid droplets in a mixture of Bose-Einstein condensates, Science **359**, 301 (2018).

[44] G. Semeghini, G. Ferioli, L. Masi, C. Mazzinghi, L. Wolswijk, F. Minardi, M. Modugno, G. Modugno, M. Inguscio, and M. Fattori, Self-Bound Quantum Droplets of Atomic Mixtures in Free Space, Phys. Rev. Lett. **120**, 235301 (2018).

[45] P. Cheiney, C. R. Cabrera, J. Sanz, B. Naylor, L. Tanzi, and L. Tarruell, Bright Soliton to Quantum Droplet Transition in a Mixture of Bose-Einstein Condensates, Phys. Rev. Lett. **120**, 135301 (2018).

[46] H. A. Haus, Higher order trapped light beam solutions, Appl. Phys. Lett. **8**, 128 (1966).

[47] V. E. Zakharov, V. V. Sobolev, and V. C. Synakh, Behavior of light beams in nonlinear media, Sov. Phys. JETP **33**, 77 (1971), http://www.jetp.ac.ru/cgi-bin/e/index/e/33/1/p77?a=list.

[48] V. I. Kruglov and R. A. Vlasov, Spiral self-trapping propagation of optical beams in media with cubic nonlinearity, Phys. Lett. A **111**, 401 (1985).

[49] G. I. Stegeman and M. Segev, Optical spatial solitons and their interactions: Universality and diversity, Science **286**, 1518 (1999).

[50] S. L. Cornish, S. T. Thompson, and C. E. Wieman, Formation of Bright Matter-Wave Solitons during the Collapse of Attractive Bose-Einstein Condensates, Phys. Rev. Lett. **96**, 170401 (2006).

[51] J. H. V. Nguyen, P. Dyke, D. Luo, B. A. Malomed, and R. G. Hulet, Collisions of matter-wave solitons, Nat. Phys. **10**, 918 (2014).

[52] G. Ferioli, G. Semeghini, L. Masi, G. Giusti, G. Modugno, M. Inguscio, A. Gallemí, A. Recati, and M. Fattori, Collisions of Self-Bound Quantum Droplets, Phys. Rev. Lett. **122**, 090401 (2019).

[53] V. M. Malkin and E. G. Shapiro, Elementary excitations for solitons of the nonlinear Schrödinger equation, Physica (Amsterdam) **53D**, 25 (1991).

[54] S. Sinha, A. Yu. Cherny, D. Kovrizhin, and J. Brand, Friction and Diffusion of Matter-Wave Bright Solitons, Phys. Rev. Lett. **96**, 030406 (2006).

[55] C.-A. Chen and C.-L. Hung, following Letter, Observation of Scale Invariance in Two-Dimensional Matter-Wave Townes Solitons, Phys. Rev. Lett. **127**, 023604 (2021).